Supporting information for "The theory of Janzen-Connell effects in corals: How dispersal and clonal growth shape pathogen-mediated coexistence"

Evan C. Johnson[1] and Sean R. Connolly[1,2]

[1]*Naos Marine Laboratories, Smithsonian Tropical Research Institute, Ancón, Panama*

[2]*College of Science and Engineering, James Cook University, Townsville, Queensland, Australia*

[*]*Corresponding author: Evan C. Johnson, JohnsonE@si.edu*

Open research statement

Code is available for peer review (figshare files here) and will be made publicly available if the paper is accepted.

Contents

Appendix S1 Supplementary figures and tables

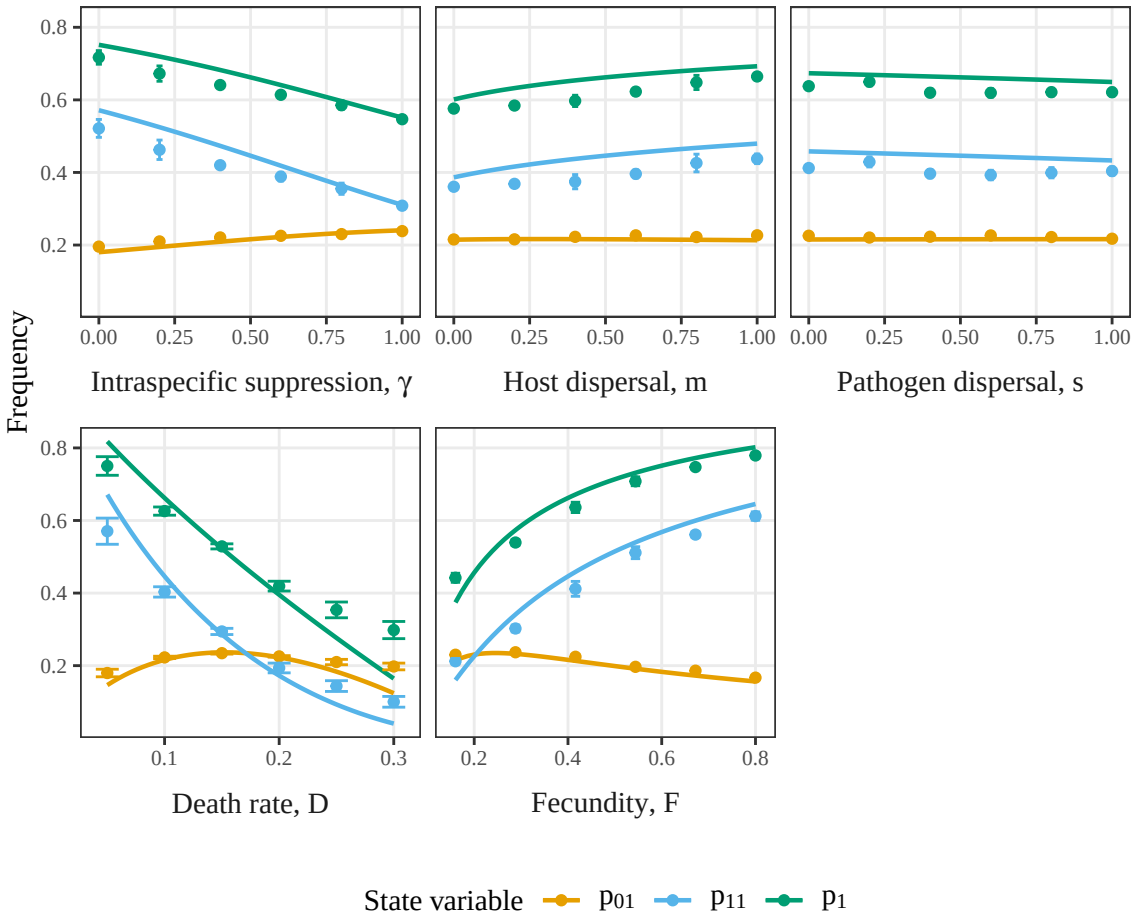

Figure S1.1: Illustration of agreement between simulations of the stochastic lattice model and the pair approximation of dynamics therein. The y-axis shows non-trivial equilibrium values of three state variables: p_{01} (empty–occupied pair frequency), p_{11} (occupied–occupied pair frequency), and p_1 (singlet frequency; overall population density). Each panel plots these equilibrium population frequencies as a function of one of five model parameters (γ, m, s, D, F). Lines show pair approximation equilibrium predictions; points show simulation results (6 values per parameter), with error bars indicating ± 1 SD of temporal variation (50 snapshots recorded every 10 time steps after a 500-step burn-in). Simulations use a 50×50 cell lattice with $\Delta t = 0.01$. Ancillary parameters: $\gamma = 0.5$, $m = 0.5$, $s = 0.5$, $D = 0.1$, $F = 0.4$, $G = 0.05$.

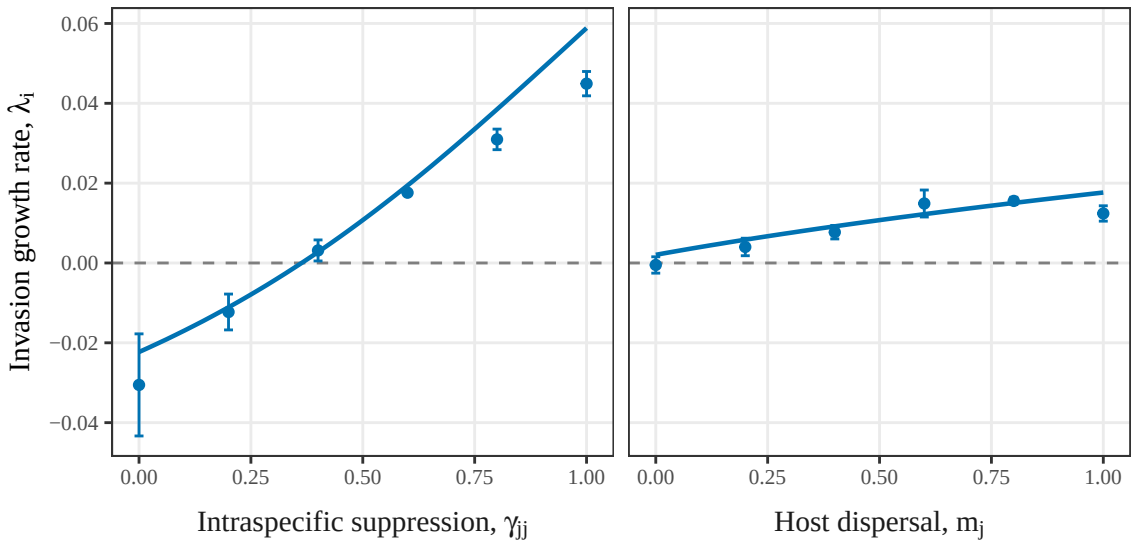

Figure S1.2: Illustration of agreement between simulations of the stochastic lattice model and the pair approximation of invasion dynamics therein. Each panel shows the invasion growth rate (λ_i) as a function of one of two model parameters (γ_{jj}, m_j). Simulations use a 100×100 cell lattice with $\Delta t = 0.1$; in each replicate, the resident equilibrates for 1000 time steps (100 time units), then the invader is introduced at 1% density. Invasion growth rate is measured after a 200-step post-introduction burn-in (20 time units, for invader spatial structure to form) and before invader density exceeds 5%. Lines show numerical pair approximation results; the dashed line indicates $\lambda_i = 0$ (invasion threshold). Points and error bars represent mean ± 1 SE of simulation results across 30 replicates. Ancillary parameters: $\gamma_{jj} = 0.5$, $m_j = 0.5$, $s = 0.5$, $D_j = 0.1$, $F_r = 0.65$, $F_i = 0.5$, $G_j = 0$, $\gamma_{ir} = \gamma_{ri} = 0$.

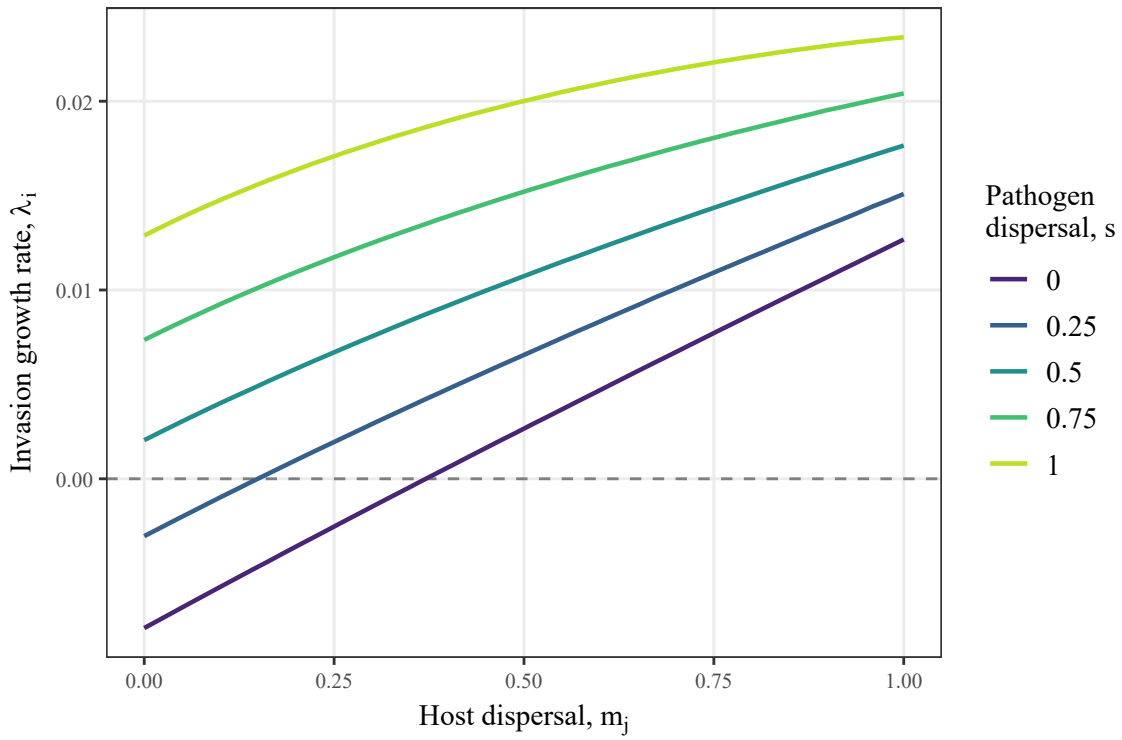

Figure S1.3: Host dispersal (m_j) and pathogen dispersal (s) both increase the invasion growth rate (λ_i), but the marginal benefit of increasing one parameter diminishes when the other is already high. This negative interaction effect can be seen as increased concave-down curvature in the λ_i versus m_j relationship at higher values of s. Pair approximation results; ancillary parameters: $F_i = 0.5$, $F_r = 0.65$; $D_i = D_r = 0.1$; $G_i = G_r = 0$; $\gamma_{ii} = \gamma_{rr} = 0.5$; $\gamma_{ir} = \gamma_{ri} = 0$.

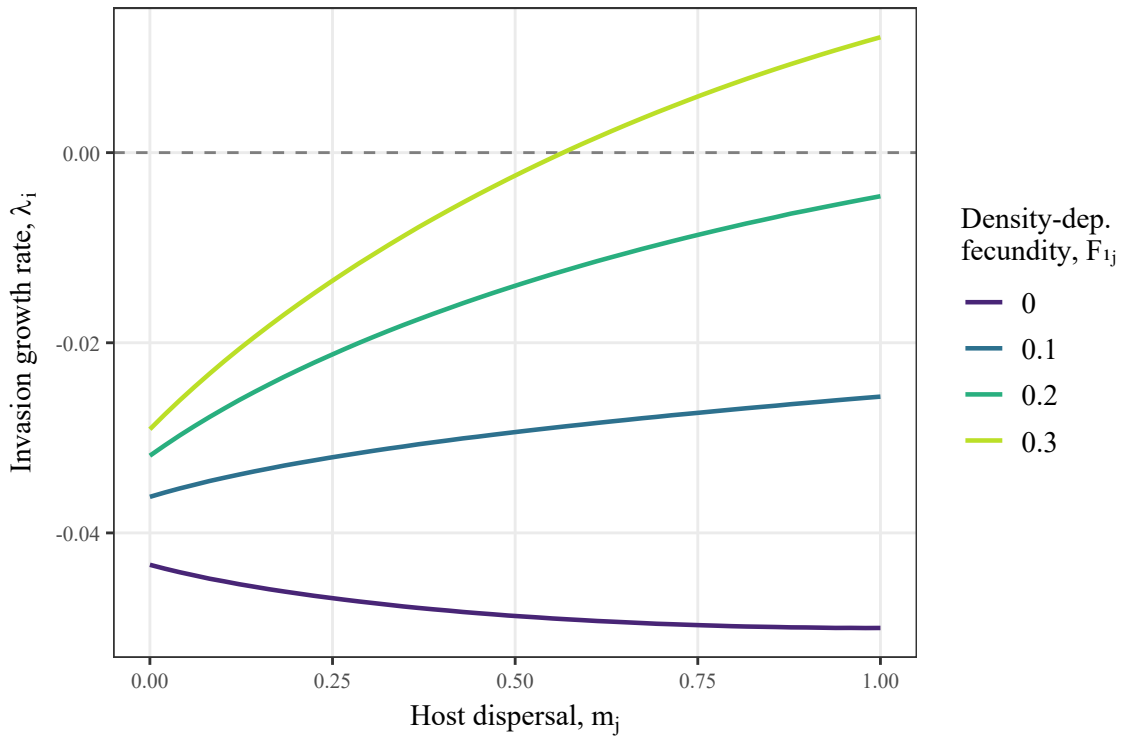

Figure S1.4: Dispersal limitation acts as an equalizing mechanism — it slows the rate of competitive exclusion in certain circumstances — but also weakens aspatial stabilizing mechanisms. Here, fecundity is density-dependent according to $F_j = F_{0j} - F_{1j}\,p_j$ (a stylized mechanism not characteristic of corals), where F_{1j} controls the strength of negative density dependence. When density dependence is absent ($F_{1j} = 0$), the equalizing effect dominates: λ_i decreases with host dispersal m_j. For sufficiently large F_{1j}, λ_i increases with m_j, demonstrating that dispersal limitation generically weakens aspatial coexistence mechanisms. Pair approximation results; ancillary parameters: $F_{0,i} = F_{0,r} = 0.3$; $D_i = 0.2$, $D_r = 0.15$; $s = 0$; $G_i = G_r = 0$; $\gamma_{ii} = \gamma_{rr} = 0$; $\gamma_{ir} = \gamma_{ri} = 0$.

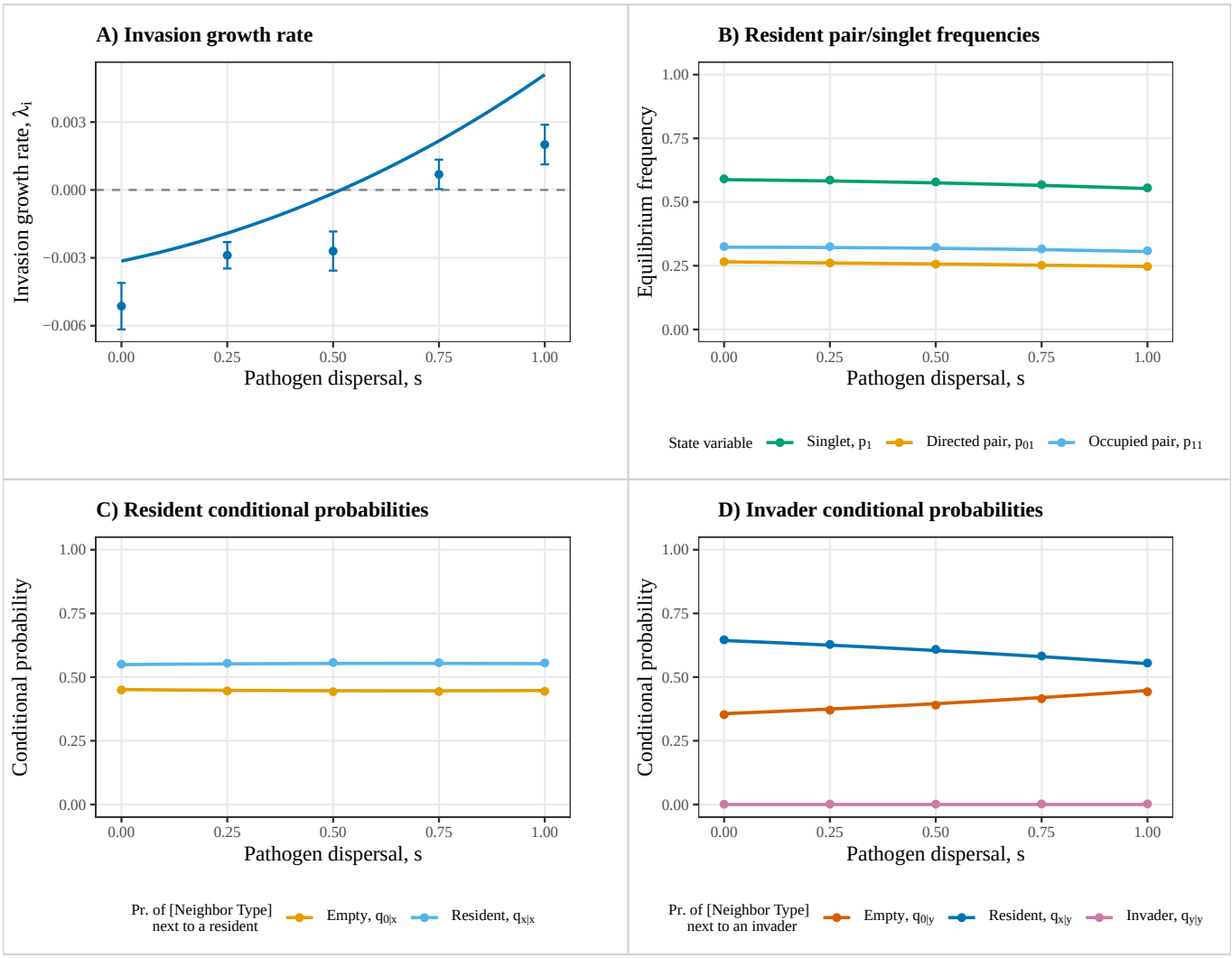

Figure S1.5: Increasing pathogen dispersal (s) reduces resident density without altering spatial structure, consistent with increased pathogen pressure on sites available for recruitment. **Panel A**: The invasion growth rate λ_i increases with s, crossing zero from negative to positive. **Panel B**: Resident singlet (p_1) and pair (p_{01}, p_{11}) frequencies at equilibrium; p_1 declines with s while relative pair structure changes little. **Panel C**: Resident conditional probabilities ($q_{0|x}$, $q_{x|x}$) are approximately flat across all values of s, confirming that spatial structure is unchanged. **Panel D**: Invader conditional probabilities as a function of s; the invader sees more empty neighbors as s increases. Lines represent pair approximation (PA) theory; points and error bars represent the mean ± 1 SE of IBM simulation results across 50 replicates. Simulations use a 200×200 cell lattice with $\Delta t = 0.1$. In each replicate, the resident equilibrates for 1000 time steps (100 time units), then the invader is introduced at 0.2% density. IGR is measured after a 100-step post-introduction burn-in (10 time units, for invader spatial structure to form) and before invader density exceeds 2%. Ancillary parameters: $m_j = 1$, $\gamma_{jj} = 1$, $D_j = 0.1$, $G_j = 0$, $F_r = 0.5$, $F_i = 0.235$, $\gamma_{ir} = \gamma_{ri} = 0$.

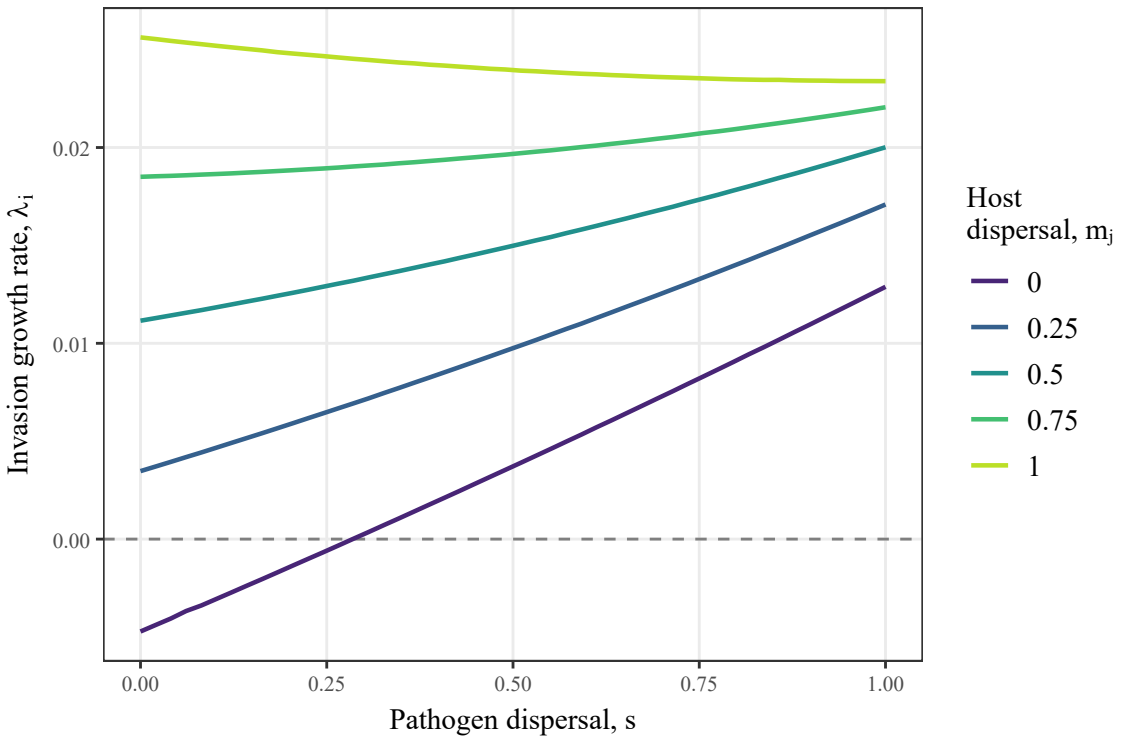

Figure S1.6: Removing pathogen self-dispersal (to the focal adult's own site) eliminates the positive effect of pathogen dispersal on coexistence under global host dispersal, supporting the explanation that local pathogens are "wasted" on occupied sites (see main text). Invasion growth rate (λ_i) as a function of pathogen dispersal (s) for different levels of host dispersal (m), using an alternative pathogen model where pathogens disperse only to z neighboring sites (denominator z instead of $z+1$). Unlike the standard model (Fig. **??**), λ_i is flat or decreasing in s when $m = 1$. Dashed line indicates $\lambda_i = 0$ (invasion threshold). Pair approximation results; ancillary parameters: $F_i = 0.5$, $F_r = 0.65$; $D_i = D_r = 0.1$; $G_i = G_r = 0$; $\gamma_{ii} = \gamma_{rr} = 0.5$; $\gamma_{ir} = \gamma_{ri} = 0$.

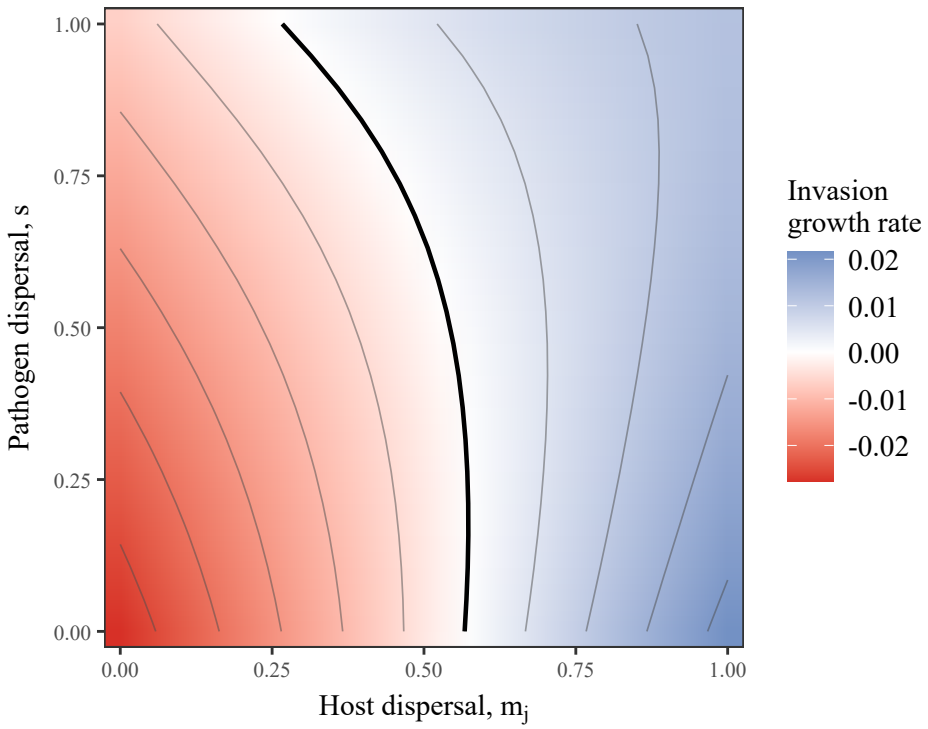

Figure S1.7: The positive effect of pathogen dispersal on coexistence largely disappears when pathogens disperse only to the z neighboring sites, excluding the focal adult's site. Invasion growth rate (λ_i) heatmap as a function of host dispersal (m_j) and pathogen dispersal (s), using an alternative pathogen model where the local suppression denominator is z instead of $z + 1$. Compare with Fig. **??**, which uses the standard model. Color scale: blue indicates positive λ_i (invasion possible), red indicates negative λ_i (invasion fails). Black contour marks $\lambda_i = 0$ (invasion threshold). Pair approximation results; ancillary parameters: $F_i = 0.25$, $F_r = 0.5$; $D_i = D_r = 0.1$; $G_i = G_r = 0$; $\gamma_{ii} = \gamma_{rr} = 1$; $\gamma_{ir} = \gamma_{ri} = 0$.

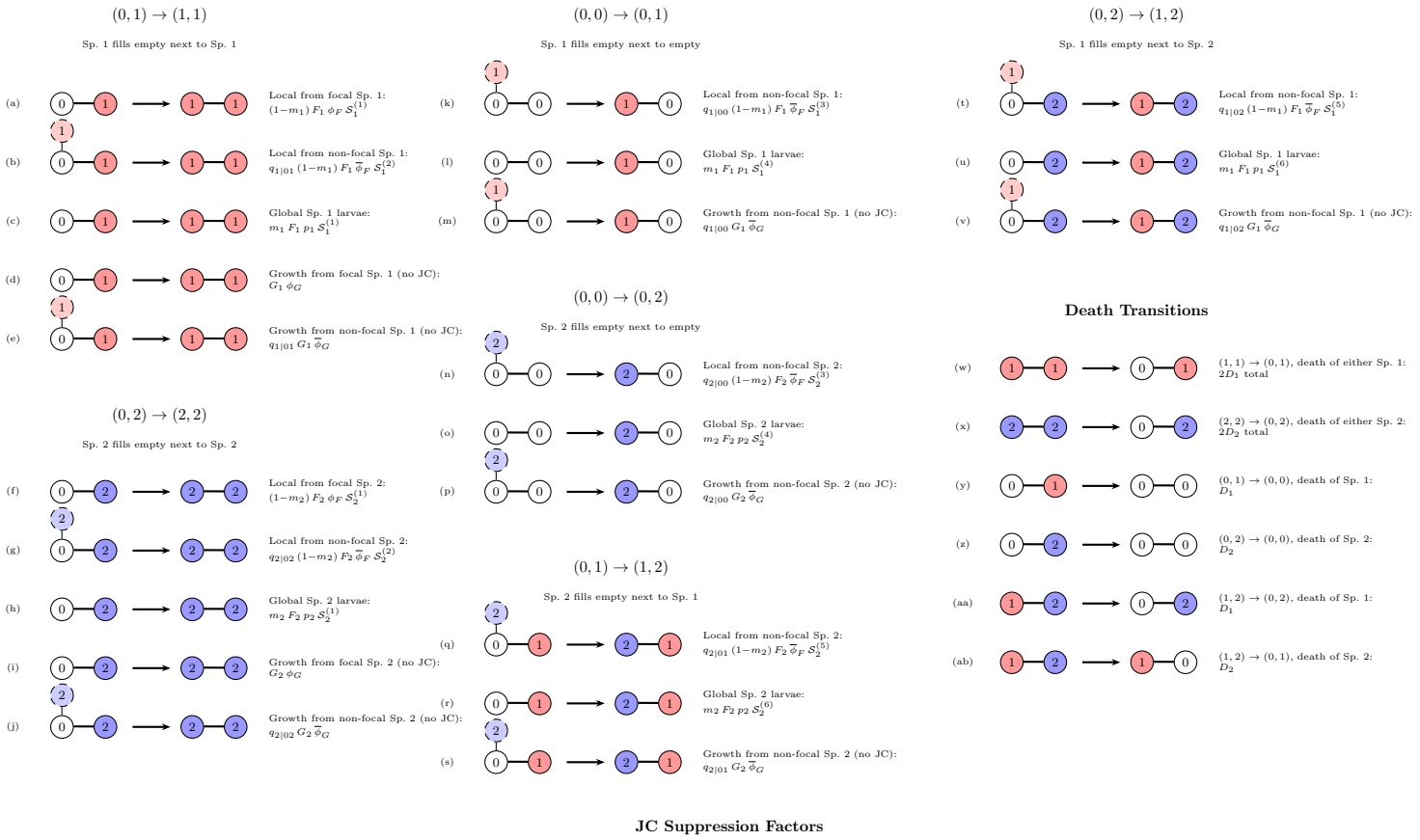

JC Suppression Factors

Species 1 Suppression Factors:

$$\mathcal{S}_1^{(1)} = 1 - \left[s(\gamma_{11}p_1 + \gamma_{12}p_2) + (1-s)\frac{\gamma_{11}[1+(z-1)q_{1|01}]+\gamma_{12}(z-1)q_{2|01}}{z+1}\right] \quad \text{(into } (0,1) \text{ from focal or global)}$$

$$\mathcal{S}_1^{(2)} = 1 - \left[s(\gamma_{11}p_1 + \gamma_{12}p_2) + (1-s)\frac{\gamma_{11}[2+(z-2)q_{1|01}]+\gamma_{12}(z-2)q_{2|01}}{z+1}\right] \quad \text{(into } (0,1) \text{ from non-focal Sp. 1)}$$

$$\mathcal{S}_1^{(3)} = 1 - \left[s(\gamma_{11}p_1 + \gamma_{12}p_2) + (1-s)\frac{\gamma_{11}[1+(z-2)q_{1|00}]+\gamma_{12}(z-2)q_{2|00}}{z+1}\right] \quad \text{(into } (0,0) \text{ from non-focal Sp. 1)}$$

$$\mathcal{S}_1^{(4)} = 1 - \left[s(\gamma_{11}p_1 + \gamma_{12}p_2) + (1-s)\frac{\gamma_{11}(z-1)q_{1|00}+\gamma_{12}(z-1)q_{2|00}}{z+1}\right] \quad \text{(into } (0,0) \text{ from global)}$$

$$\mathcal{S}_1^{(5)} = 1 - \left[s(\gamma_{11}p_1 + \gamma_{12}p_2) + (1-s)\frac{\gamma_{11}[1+(z-2)q_{1|02}]+\gamma_{12}[1+(z-2)q_{2|02}]}{z+1}\right] \quad \text{(into } (0,2) \text{ from non-focal Sp. 1)}$$

$$\mathcal{S}_1^{(6)} = 1 - \left[s(\gamma_{11}p_1 + \gamma_{12}p_2) + (1-s)\frac{\gamma_{11}(z-1)q_{1|02}+\gamma_{12}[1+(z-1)q_{2|02}]}{z+1}\right] \quad \text{(into } (0,2) \text{ from global)}$$

Figure S1.8: Complete enumeration of all local transitions affecting pair configurations in the two-species model. **Left column**: Transitions converting $(0,1) \to (1,1)$ (species 1 fills empty next to conspecific, rows a–e) and $(0,2) \to (2,2)$ (species 2 fills empty next to conspecific, rows f–j). **Middle column**: Transitions converting $(0,0) \to (0,1)$ or $(0,2)$ (either species fills empty next to empty, rows k–p) and $(0,1) \to (1,2)$ (species 2 fills empty next to heterospecific, rows q–s). **Right column**: Transitions converting $(0,2) \to (1,2)$ (species 1 fills empty next to heterospecific, rows t–v) and all death transitions (rows w–ab).

Appendix S2 Two-Species Pair Dynamics

This appendix provides a derivation of the pair approximation equations for the two-species Janzen-Connell model. We derive all suppression factors, recruitment and growth rates, and assemble the complete system of differential equations.

S2.1 General Structure of Two-Species Suppression

In the two-species model, the suppression experienced by a recruiting larva of species i depends on the weighted contributions of both conspecific and heterospecific neighbors, with weights determined by the suppression matrix $\boldsymbol{\gamma}$. Recall that the general recruitment probability for species i landing at an empty site with κ_1 species-1 neighbors and κ_2 species-2 neighbors is

$$\text{Recruitment prob.} = \left(1 - \left[s(\gamma_{i1}p_1 + \gamma_{i2}p_2) + (1-s)\frac{\gamma_{i1}\kappa_1 + \gamma_{i2}\kappa_2}{z+1}\right]\right). \tag{S2.1}$$

When deriving pair dynamics, we must compute expected suppression over uncertain neighborhood configurations. The suppression factor for a given recruitment context takes the general form

$$S = 1 - \left[s(\gamma_{i1}p_1 + \gamma_{i2}p_2) + (1-s)\frac{\gamma_{i1}\mathbb{E}[\kappa_1] + \gamma_{i2}\mathbb{E}[\kappa_2]}{z+1}\right], \tag{S2.2}$$

where $\mathbb{E}[\kappa_1]$ and $\mathbb{E}[\kappa_2]$ denote the expected number of species-1 and species-2 neighbors, respectively. Unlike the single-species case, we must now compute expected neighbor counts for both species in each recruitment context, leading to six distinct suppression factors per species.

The expected number of neighbors of each species is computed by decomposing neighbors into "certain" neighbors, whose states are determined by the pair configuration or larval source, and "uncertain" neighbors, whose states follow conditional probabilities. For a focal empty site in a $(0, j)$ pair, there are z neighbors in total: one focal neighbor (in state j) and $z-1$ non-focal neighbors. Certain neighbors include the focal neighbor, whose state is known from the pair type, and—if recruitment originates from a non-focal conspecific—the larval source. Uncertain neighbors are the remaining non-focal sites, whose species composition follows the conditional probabilities $q_{1|0} = p_{01}/p_0$ and $q_{2|0} = p_{02}/p_0$ under the pair approximation. The

expected neighbor counts are therefore:

$$\mathbb{E}[\kappa_1] = (\text{certain species-1 neighbors}) + (\text{uncertain neighbors}) \times q_{1|0} \tag{S2.3}$$

$$\mathbb{E}[\kappa_2] = (\text{certain species-2 neighbors}) + (\text{uncertain neighbors}) \times q_{2|0} \tag{S2.4}$$

S2.2 Suppression Factors

Species 1 recruiting into $(0,1)$ pairs (adjacent to conspecific). The suppression factor $\mathcal{S}_1^{(1)}$ applies when larvae arrive from the focal conspecific or from the global pool. There is 1 certain species-1 neighbor (the focal conspecific), 0 certain species-2 neighbors, and $z-1$ uncertain non-focal neighbors. The expected neighbor counts are $\mathbb{E}[\kappa_1] = 1 + (z-1)q_{1|01}$ and $\mathbb{E}[\kappa_2] = (z-1)q_{2|01}$, which results in the suppression factor

$$\mathcal{S}_1^{(1)} = 1 - \left[s(\gamma_{11}p_1 + \gamma_{12}p_2) + (1-s)\frac{\gamma_{11}[1 + (z-1)q_{1|01}] + \gamma_{12}(z-1)q_{2|01}}{z+1} \right]. \tag{S2.5}$$

The suppression factor $\mathcal{S}_1^{(2)}$ applies when larvae arrive from a non-focal conspecific. There are 2 certain species-1 neighbors (the focal conspecific plus the larval source), 0 certain species-2 neighbors, and $z-2$ uncertain non-focal neighbors. The expected counts are $\mathbb{E}[\kappa_1] = 2 + (z-2)q_{1|01}$ and $\mathbb{E}[\kappa_2] = (z-2)q_{2|01}$, which results in the suppression factor

$$\mathcal{S}_1^{(2)} = 1 - \left[s(\gamma_{11}p_1 + \gamma_{12}p_2) + (1-s)\frac{\gamma_{11}[2 + (z-2)q_{1|01}] + \gamma_{12}(z-2)q_{2|01}}{z+1} \right]. \tag{S2.6}$$

Species 1 recruiting into $(0,0)$ pairs (adjacent to empty). The suppression factor $\mathcal{S}_1^{(3)}$ applies when larvae arrive from a non-focal conspecific. There is 1 certain species-1 neighbor (the larval source), 0 certain species-2 neighbors, and $z-2$ uncertain non-focal neighbors. The expected counts are $\mathbb{E}[\kappa_1] = 1 + (z-2)q_{1|00}$ and $\mathbb{E}[\kappa_2] = (z-2)q_{2|00}$, which results in

$$\mathcal{S}_1^{(3)} = 1 - \left[s(\gamma_{11}p_1 + \gamma_{12}p_2) + (1-s)\frac{\gamma_{11}[1 + (z-2)q_{1|00}] + \gamma_{12}(z-2)q_{2|00}}{z+1} \right]. \tag{S2.7}$$

The suppression factor $\mathcal{S}_1^{(4)}$ applies when larvae arrive from the global pool. There are 0 certain species-1 neighbors, 0 certain species-2 neighbors, and $z-1$ uncertain non-focal neighbors. The expected counts are $\mathbb{E}[\kappa_1] = (z-1)q_{1|00}$ and $\mathbb{E}[\kappa_2] = (z-1)q_{2|00}$, which results in

$$\mathcal{S}_1^{(4)} = 1 - \left[s(\gamma_{11}p_1 + \gamma_{12}p_2) + (1-s)\frac{\gamma_{11}(z-1)q_{1|00} + \gamma_{12}(z-1)q_{2|00}}{z+1} \right]. \tag{S2.8}$$

Species 1 recruiting into $(0,2)$ pairs (adjacent to heterospecific). The suppression factor $\mathcal{S}_1^{(5)}$ applies when larvae arrive from a non-focal conspecific. There is 1 certain species-1 neighbor (the larval source), 1 certain species-2 neighbor (the focal heterospecific), and $z-2$ uncertain non-focal neighbors. The expected counts are $\mathbb{E}[\kappa_1] = 1 + (z-2)q_{1|02}$ and $\mathbb{E}[\kappa_2] = 1 + (z-2)q_{2|02}$, which results in

$$\mathcal{S}_1^{(5)} = 1 - \left[s(\gamma_{11}p_1 + \gamma_{12}p_2) + (1-s)\frac{\gamma_{11}[1+(z-2)q_{1|02}] + \gamma_{12}[1+(z-2)q_{2|02}]}{z+1} \right]. \quad \text{(S2.9)}$$

The suppression factor $\mathcal{S}_1^{(6)}$ applies when larvae arrive from the global pool. There are 0 certain species-1 neighbors, 1 certain species-2 neighbor (the focal heterospecific), and $z-1$ uncertain non-focal neighbors. The expected counts are $\mathbb{E}[\kappa_1] = (z-1)q_{1|02}$ and $\mathbb{E}[\kappa_2] = 1 + (z-1)q_{2|02}$, which results in

$$\mathcal{S}_1^{(6)} = 1 - \left[s(\gamma_{11}p_1 + \gamma_{12}p_2) + (1-s)\frac{\gamma_{11}(z-1)q_{1|02} + \gamma_{12}[1+(z-1)q_{2|02}]}{z+1} \right]. \quad \text{(S2.10)}$$

The six suppression factors for species 2 follow by interchanging species indices. Specifically, $\mathcal{S}_2^{(1)}$ and $\mathcal{S}_2^{(2)}$ apply to recruitment into $(0,2)$ pairs and use conditional probabilities $q_{1|02}$ and $q_{2|02}$; $\mathcal{S}_2^{(3)}$ and $\mathcal{S}_2^{(4)}$ apply to recruitment into $(0,0)$ pairs and use $q_{1|00}$ and $q_{2|00}$; $\mathcal{S}_2^{(5)}$ and $\mathcal{S}_2^{(6)}$ apply to recruitment into $(0,1)$ pairs and use $q_{1|01}$ and $q_{2|01}$.

S2.3 Recruitment and Growth Rates

The recruitment rates combine contributions from local and global larval sources, each weighted by the appropriate suppression factor and conditional probability. For species 1 recruiting into $(0,1)$ pairs, local larvae arrive from both the focal conspecific and non-focal conspecifics, while global larvae arrive from the larval pool:

$$\mathcal{R}_{01}^{(1)} = \mathcal{S}_1^{(1)}\left[(1-m_1)\,F_1\,\phi_F + m_1\,F_1\,p_1\right] + \mathcal{S}_1^{(2)}\,(1-m_1)\,F_1\,\overline{\phi}_F\,q_{1|01}. \quad \text{(S2.11)}$$

For recruitment into $(0,0)$ pairs, there is no focal conspecific contribution:

$$\mathcal{R}_{00}^{(1)} = \mathcal{S}_1^{(3)}\,(1-m_1)\,F_1\,\overline{\phi}_F\,q_{1|00} + \mathcal{S}_1^{(4)}\,m_1\,F_1\,p_1. \quad \text{(S2.12)}$$

For recruitment into $(0,2)$ pairs, the focal neighbor is a heterospecific and cannot contribute conspecific larvae:

$$\mathcal{R}_{02}^{(1)} = \mathcal{S}_1^{(5)}\,(1-m_1)\,F_1\,\overline{\phi}_F\,q_{1|02} + \mathcal{S}_1^{(6)}\,m_1\,F_1\,p_1. \tag{S2.13}$$

The recruitment rates for species 2 follow the same structure:

$$\mathcal{R}_{02}^{(2)} = \mathcal{S}_2^{(1)}\,[(1-m_2)\,F_2\,\phi_F + m_2\,F_2\,p_2] + \mathcal{S}_2^{(2)}\,(1-m_2)\,F_2\,\overline{\phi}_F\,q_{2|02} \tag{S2.14}$$

$$\mathcal{R}_{00}^{(2)} = \mathcal{S}_2^{(3)}\,(1-m_2)\,F_2\,\overline{\phi}_F\,q_{2|00} + \mathcal{S}_2^{(4)}\,m_2\,F_2\,p_2 \tag{S2.15}$$

$$\mathcal{R}_{01}^{(2)} = \mathcal{S}_2^{(5)}\,(1-m_2)\,F_2\,\overline{\phi}_F\,q_{2|01} + \mathcal{S}_2^{(6)}\,m_2\,F_2\,p_2. \tag{S2.16}$$

The growth rates are not subject to Janzen-Connell suppression. For species 1, growth into $(0,1)$ pairs includes contributions from both the focal conspecific and non-focal conspecifics:

$$\mathcal{G}_{01}^{(1)} = G_1\left(\phi_G + \overline{\phi}_G\,q_{1|01}\right). \tag{S2.17}$$

Growth into $(0,0)$ pairs includes only contributions from non-focal conspecifics:

$$\mathcal{G}_{00}^{(1)} = G_1\,\overline{\phi}_G\,q_{1|00}. \tag{S2.18}$$

Growth into $(0,2)$ pairs similarly includes only contributions from non-focal conspecifics:

$$\mathcal{G}_{02}^{(1)} = G_1\,\overline{\phi}_G\,q_{1|02}. \tag{S2.19}$$

Note that unlike the post-pair-approximation forms, $\mathcal{G}_{00}^{(1)} \neq \mathcal{G}_{02}^{(1)}$ because the conditional probabilities $q_{1|00}$ and $q_{1|02}$ may differ.

The growth rates for species 2 follow by symmetry:

$$\mathcal{G}_{02}^{(2)} = G_2\left(\phi_G + \overline{\phi}_G\,q_{2|02}\right) \tag{S2.20}$$

$$\mathcal{G}_{00}^{(2)} = G_2\,\overline{\phi}_G\,q_{2|00} \tag{S2.21}$$

$$\mathcal{G}_{01}^{(2)} = G_2\,\overline{\phi}_G\,q_{2|01}. \tag{S2.22}$$

S2.4 Assembly of the Differential Equations

The differential equations for pair frequencies are derived by enumerating all transitions that create or destroy each pair type. Figure S1.8 displays the complete set of transitions for the two-species model, organized by pair type and demographic process. Combining all transitions yields the following system of five differential equations:

$$\frac{\mathrm{d}p_{01}}{\mathrm{d}t} = D_1 p_{11} + D_2 p_{12} + p_{00}(\mathcal{R}_{00}^{(1)} + \mathcal{G}_{00}^{(1)}) - D_1 p_{01} - p_{01}\left[(\mathcal{R}_{01}^{(1)} + \mathcal{G}_{01}^{(1)}) + (\mathcal{R}_{01}^{(2)} + \mathcal{G}_{01}^{(2)})\right] \tag{S2.23}$$

$$\frac{\mathrm{d}p_{02}}{\mathrm{d}t} = D_2 p_{22} + D_1 p_{12} + p_{00}(\mathcal{R}_{00}^{(2)} + \mathcal{G}_{00}^{(2)}) - D_2 p_{02} - p_{02}\left[(\mathcal{R}_{02}^{(2)} + \mathcal{G}_{02}^{(2)}) + (\mathcal{R}_{02}^{(1)} + \mathcal{G}_{02}^{(1)})\right] \tag{S2.24}$$

$$\frac{\mathrm{d}p_{11}}{\mathrm{d}t} = 2p_{01}(\mathcal{R}_{01}^{(1)} + \mathcal{G}_{01}^{(1)}) - 2D_1 p_{11} \tag{S2.25}$$

$$\frac{\mathrm{d}p_{22}}{\mathrm{d}t} = 2p_{02}(\mathcal{R}_{02}^{(2)} + \mathcal{G}_{02}^{(2)}) - 2D_2 p_{22} \tag{S2.26}$$

$$\frac{\mathrm{d}p_{12}}{\mathrm{d}t} = p_{01}(\mathcal{R}_{01}^{(2)} + \mathcal{G}_{01}^{(2)}) + p_{02}(\mathcal{R}_{02}^{(1)} + \mathcal{G}_{02}^{(1)}) - (D_1 + D_2)p_{12}. \tag{S2.27}$$

These equations are not closed because the script-letter rates ($\mathcal{R}$, $\mathcal{G}$)—which signal dependence on triplet-level conditional probabilities $q_{k|ij}$—cannot be expressed purely in terms of pair frequencies; recall that $q_{k|ij} = p_{kij}/p_{ij}$, where p_{kij} is the frequency of triplet configurations with a central site in state i, one neighbor in state j, and another neighbor in state k.

We apply the standard pair approximation by replacing $q_{k|ij}$ with $q_{k|i} = p_{ik}/p_i$ for all pair types (i, j). Under this approximation, the growth rates satisfy $\mathcal{G}_{00}^{(1)} = \mathcal{G}_{02}^{(1)}$ and $\mathcal{G}_{00}^{(2)} = \mathcal{G}_{01}^{(2)}$ under the pair approximation, since the contribution from non-focal neighbors no longer depends on the focal neighbor's state.

The effective demographic rates under the pair approximation are denoted with roman

letters (i.e., $\mathcal{R} \to R$, $\mathcal{G} \to G$, $\mathcal{S} \to S$):

$$R_{01}^{(1)} = S_1^{(1)} \left[(1-m_1)\, F_1\, \phi_F + m_1\, F_1\, p_1\right] + S_1^{(2)}\, (1-m_1)\, F_1\, \overline{\phi}_F\, q_{1|0} \tag{S2.28}$$

$$R_{00}^{(1)} = S_1^{(3)}\, (1-m_1)\, F_1\, \overline{\phi}_F\, q_{1|0} + S_1^{(4)}\, m_1\, F_1\, p_1 \tag{S2.29}$$

$$R_{02}^{(1)} = S_1^{(5)}\, (1-m_1)\, F_1\, \overline{\phi}_F\, q_{1|0} + S_1^{(6)}\, m_1\, F_1\, p_1 \tag{S2.30}$$

$$G_{01}^{(1)} = G_1 \left(\phi_G + \overline{\phi}_G\, q_{1|0}\right) \tag{S2.31}$$

$$G_{00}^{(1)} = G_{02}^{(1)} = G_1\, \overline{\phi}_G\, q_{1|0} \tag{S2.32}$$

with analogous expressions for species 2 (obtained by interchanging species indices). The suppression factors $S_i^{(k)}$ are the pair-approximation versions of $\mathcal{S}_i^{(k)}$, with all conditional probabilities replaced by $q_{1|0}$ and $q_{2|0}$. The full system can then be written as Eq. **??**–Eq. **??** in the main text.

The empty pair frequency follows from the normalization constraint

$$p_{00} = 1 - 2p_{01} - 2p_{02} - p_{11} - 2p_{12} - p_{22}. \tag{S2.33}$$

Appendix S3 Perturbation theory

S3.1 Setup

The invasion growth rate is approximated with an expansion in two parameters about zero: the recruitment suppression parameter γ and the reciprocal of the number of neighbors $\epsilon = 1/z$. The zeroth order gives the mean-field limit: $\gamma = 0$ and $\epsilon = 0$ correspond to no JC effects and infinite connectivity, thus all pair frequencies become products of singlet frequencies (i.e., $p_{01} = p_1(1-p_1)$, $p_{11} = p_1^2$), and $q_{1|0} = p_1$. For analytical tractability, the perturbation analysis imposes the following simplifying assumptions beyond those of the full pair approximation: (i) species are symmetric, sharing demographic parameters D, F, m, and G; (ii) clonal growth is absent ($G = 0$); (iii) heterospecific suppression is absent ($\gamma_{ij} = 0$ for $i \neq j$), so only conspecific pathogens suppress recruitment; and (iv) both species share the same conspecific suppression intensity $\gamma_{ii} = \gamma$.

S3.1.1 Mean-field equilibrium

In the mean-field limit ($\gamma = 0$, $\epsilon = 0$), the resident equilibrium density is simply $p_1^{(0)} = 1 - D/F$. When JC suppression is present ($\gamma > 0$) but connectivity remains infinite ($\epsilon = 0$), the nontrivial single-species equilibrium is

$$p_1^* = \frac{1 + \gamma - \sqrt{(\gamma - 1)^2 + 4D\gamma/F}}{2\gamma}. \tag{S3.1}$$

S3.1.2 Eigenvalue perturbation

The perturbation approach requires that both the resident equilibrium and Jacobian also be expanded in powers of γ and ϵ: the resident pair frequencies take the form $p_{0r} = p_{0r}^{(00)} + \gamma p_{0r}^{(10)} + \epsilon p_{0r}^{(01)} + \ldots$, with an analogous expansion for p_{rr}, and the Jacobian is expanded as $\mathbf{J} = \mathbf{J}^{(00)} + \gamma \mathbf{J}^{(10)} + \epsilon \mathbf{J}^{(01)} + \ldots$, where corrections to $\mathbf{J}$ arise both from changes in the resident equilibrium and from the direct dependence of transition rates on γ and ϵ.

Eigenvalue perturbation theory (Kato, 1995, pp. 79–81) relates the coefficients $\lambda^{(ij)}$ to corrections in the Jacobian and, at higher orders, to corrections in the eigenvectors. At zeroth order, the dominant eigenvalue $\lambda^{(00)}$ is obtained directly as the eigenvalue with largest real part of the unperturbed Jacobian $\mathbf{J}^{(00)}$. Let $\mathbf{v}$ and $\mathbf{w}$ denote the corresponding right and left eigenvectors, respectively, normalized such that $\mathbf{w} \cdot \mathbf{v} = 1$. First-order corrections are computed by projecting the first-order Jacobian perturbations onto the dominant eigenspace:

$$\lambda^{(10)} = \mathbf{w} \cdot \mathbf{J}^{(10)} \cdot \mathbf{v}, \quad \lambda^{(01)} = \mathbf{w} \cdot \mathbf{J}^{(01)} \cdot \mathbf{v}. \tag{S3.2}$$

For a simple eigenvalue, the second-order correction follows Kato's biorthogonal left/right eigenvector formula (Kato, 1995, Eq. (2.36), p. 81). Second-order eigenvalue corrections incorporate both the direct contribution from the second-order Jacobian perturbation and an indirect contribution mediated by the first-order eigenvector correction:

$$\lambda^{(20)} = \mathbf{w} \cdot \mathbf{J}^{(20)} \cdot \mathbf{v} + \mathbf{w} \cdot \mathbf{J}^{(10)} \cdot \mathbf{v}^{(10)}, \tag{S3.3}$$

with analogous expressions for $\lambda^{(02)}$ and the mixed term $\lambda^{(11)}$. The requisite first-order eigenvector correction $\mathbf{v}^{(10)}$ captures how the dominant eigenvector shifts in response to $\mathbf{J}^{(10)}$. This

correction is computed as

$$\mathbf{v}^{(10)} = \sum_{k \neq 0} \frac{\mathbf{w}_k \cdot \mathbf{J}^{(10)} \cdot \mathbf{v}}{\left(\lambda^{(00)} - \lambda_k\right)\left(\mathbf{w}_k \cdot \mathbf{v}_k\right)} \mathbf{v}_k, \tag{S3.4}$$

where the sum runs over all non-dominant eigenvectors $\mathbf{v}_k$ with corresponding left eigenvectors $\mathbf{w}_k$ and eigenvalues λ_k.

S3.2 Results

All symbolic calculations below were performed in *Mathematica* (Wolfram Research, Inc., 2024; see `mathematica/jc_pa_analytical.nb` in the supporting files). The β form of the invasion growth rate (Eq. **??**) involves two approximations. First, the invasion growth rate is expanded through second order in γ and ϵ, yielding coefficients $\lambda^{(ij)}$ that are exact polynomial functions of m, s, D, and F (some of degree four or higher in m). Second, and because analytical expressions could not be attained otherwise, these polynomials are Taylor-expanded about $m = 0$, $s = 0$ through second order. The combined approximation is

$$\lambda \approx \beta_0 + \beta_m\, m + \beta_s\, s - \beta_{mm}\, m^2 - \beta_{ms}\, m\, s. \tag{S3.5}$$

Each β coefficient receives contributions from multiple perturbation orders (i.e., different powers of γ and ϵ). The expressions below give the lowest-order contribution to each coefficient — the term with the smallest combined power of γ and ϵ. No s^2 term appears because s enters the perturbation only through the $\gamma\epsilon$ cross-term $\lambda^{(11)}$, which contributes at most linearly in s at this order.

The coefficients β_s and β_{ms} arise entirely from the $\gamma\epsilon$ cross-term $\lambda^{(11)}$ and are therefore exact at this perturbation order:

$$\beta_s = \frac{D\gamma\epsilon\,(3F + D)(F - D)}{F^2}, \tag{S3.6}$$

$$\beta_{ms} = \frac{D\gamma\epsilon\,(2F + D)(F - D)}{F^2}. \tag{S3.7}$$

Both are manifestly positive for $F > D > 0$, confirming that pathogen dispersal promotes coexistence ($\beta_s > 0$) and that increasing pathogen dispersal reduces the marginal benefit of host dispersal ($\beta_{ms} > 0$). That both coefficients require $\epsilon > 0$ (i.e., finite z) reflects the fact

that pathogen dispersal mode is irrelevant in the mean-field limit.

The remaining coefficients receive their leading contributions at $O(\gamma)$ or $O(\gamma\epsilon)$. Host-dispersal mode is irrelevant in the mean-field limit, so the host-dispersal coefficients are read from the spatial cross-term rather than from the pure γ^2 term:

$$\beta_0 \approx \frac{D\gamma(F-D)}{F}, \tag{S3.8}$$

$$\beta_m \approx \frac{D\gamma\epsilon\,(D+2F)(D^2-DF+2F^2)}{F^2(D+F)}, \tag{S3.9}$$

$$\beta_{mm} \approx \frac{D\gamma\epsilon\,(D^3+D^2F-DF^2+F^3)}{F^2(D+F)}. \tag{S3.10}$$

All three are positive for $F > D > 0$: $D^2 - DF + 2F^2 > 0$, and $D^3 + D^2F - DF^2 + F^3 = D^2(D+F) + F^2(F-D) > 0$. The shared $O(\gamma\epsilon)$ scaling of β_m, β_s, β_{mm}, and β_{ms} shows that dispersal-mode effects arise from the interaction between JC suppression and finite spatial neighborhoods.

References

Kato, T. (1995). *Perturbation Theory for Linear Operators*, volume 132 of *Classics in Mathematics*. Springer, Berlin, 2nd edition.

Wolfram Research, Inc. (2024). Mathematica, version 14.1.